

# MURMR: A Multimodal Sensing Framework for Automated Group Behavior Analysis in Mixed Reality

Diana Romero\*

dgromer1@uci.edu

University of California, Irvine

Yasra Chandio\*

ychandio@umass.edu

University of Massachusetts Amherst

Fatima M. Anwar

fanwar@umass.edu

University of Massachusetts Amherst

Salma Elmalaki

salma.elmalaki@uci.edu

University of California, Irvine

## ABSTRACT

Collaboration is at the heart of many complex tasks, and mixed reality (MR) offers a powerful new medium to support it. Understanding how teams coordinate in immersive environments is critical for designing effective MR applications that support collaborative work. However, existing methods rely on external observation systems and manual annotation, lacking deployable solutions for capturing temporal collaboration dynamics. We present MURMR, a system with two complementary modules that passively analyze multimodal interaction data from commodity MR headsets. Our structural analysis module constructs automated sociograms revealing group organization and roles, while our temporal analysis module performs unsupervised clustering to identify moment-to-moment dyad behavior patterns. Through a 48-participant study with egocentric video validation, we demonstrate that the structural module captures stable interaction patterns while the temporal module reveals substantial behavioral variability that session-level approaches miss. This dual-module architecture advances collaboration research by establishing that structural and temporal dynamics require separate analytical approaches, enabling both real-time group monitoring and detailed behavioral understanding in immersive collaborative environments.

**Index Terms:** Mixed Reality, Collaboration, Sensing

## 1 INTRODUCTION

Collaborative Mixed Reality (MR) applications are transforming fields such as surgical planning and training [20], shared 3D architectural walkthroughs [13], remote industrial equipment maintenance guidance [21], and co-creative product prototyping [8], each relying on seamless coordination among multiple users (in real time). However, despite these rich, group-based scenarios, we still lack scalable, real-time methods to observe and analyze how groups interact in immersive technologies. Effective collaboration depends on participants' communication patterns, decision-making, turn-taking, social norm setting, and authority negotiation [19, 31], all of which vary with group size, composition, and task complexity [22, 25] and ultimately shape productivity, creativity, and performance [49, 61]. While traditional research has examined group behavior in physical settings, the emergence of immersive technologies (AR/VR/MR) offers new frontiers for collaborative work.

\*Diana Romero and Yasra Chandio contributed equally to this work as co-first authors.

MR, in particular, seamlessly integrates digital objects into the physical environment, enabling interaction as if they were physically present. This seamless integration creates collaborative scenarios distinct from VR (fully immersive) or AR (digital overlay), introducing novel social and spatial variables such as spatial awareness [37, 42], presence [28, 64], and multimodal communication [40, 62]. Moreover, inter-, intra-, and multi-user variability [15, 76] demands methods that can capture and interpret these complex, evolving interactions. Previous research has significantly advanced our understanding of collaboration through various methods, including VR/AR teams [75], sociometric badges [32], and external techniques such as motion capture cameras, intrusive wearable sensors, or manual video analysis [74]. However, these approaches cannot be applied directly to the MR headset environment on the device [16]. Since MR uniquely blends physical and virtual worlds, it leads to challenges such as occlusions and spatial constraints. In this context, the aforementioned methods are unable to capture crucial *in situ* cues such as gaze, speech, and motion, which are essential to understand group behavior [2].

In this paper, we address the need for a deeper understanding of group behavior in MR by answering the following research questions (**RQ**): *How can the sensory systems in MR headsets effectively capture group behavior during collaborative tasks?* (**RQ1**) and *What algorithms can process and interpret the data to infer group behavior?* (**RQ2**). To answer these, we introduce **Multimodal Unsupervised Relational MR (MURMR)**, a novel framework to integrate passive, multimodal sensing from commodity MR headsets to automate the inference of group interaction dynamics both structurally and temporally. Our contributions are:

1. A *Passive Multimodal Sensing Pipeline* that captures and processes raw gaze, audio, and motion data from commodity MR headsets without external hardware, thus preserving natural interaction.
2. A novel *Structural Analysis Module* that automatically translates multimodal sensor streams into weighted sociograms and computes network metrics across multiple temporal granularities, enabling both session-level and dynamic windowed analysis of group interaction patterns.
3. An *Unsupervised Temporal Clustering Module* that identifies distinct, evolving phases of group behavior from the aggregated sociograms without requiring manual annotation or pre-labeled data.
4. An *Empirical Validation* via a human subject study ( $N = 48$ ) that confirms the framework's technical stability and, more importantly, reveals meaningful and interpretable group dynamics, demonstrating its utility for collaboration analysis.

Table 1: Comparative analysis of related works across key dimensions of collaborative MR analytics. Each column captures a distinct capability, ranging from higher-order collaboration constructs to technical support for replay and open pipelines. Symbols denote the level of support: ● = present, ◉ = partially present or limited, ○ = absent.

Work	Collab. metrics	Auto. metrics	Unsupervised inference	Headset-only	Real-time	Group-level	Subgroups detection	Multi-user	Replay env.	Manual coding	Open formats
<b>MURMR (ours)</b>	●	●	●	●	◉	●	●	●	○	○	◉
Yang (2022) [71]	●	○	○	●	○	●	○	◉	○	●	○
Echeverria (2019) [14]	●	◉	○	○	○	●	◉	●	◉	●	○
PLUME (2024) [30]	○	○	○	◉	○	○	○	○	●	●	●
ISA (2024) [35]	◉	◉	○	○	○	●	◉	●	●	●	○
RELIVE (2022) [27]	○	○	○	◉	○	◉	○	●	●	●	◉
MIRIA (2021) [7]	○	○	○	○	○	◉	○	●	●	○	○
AUTOVis (2023) [29]	○	○	○	○	○	◉	○	◉	●	●	◉
TESSERACT (2023) [39]	○	○	○	○	○	○	○	○	●	○	○
PSI (2021) [1]	○	○	○	○	◉	○	○	●	●	●	◉
MRAT (2020) [47]	○	○	○	◉	○	◉	○	●	●	●	○

## 2 RELATED WORK

### 2.1 Group Behavior Sensing in MR

Decades of VR research have revealed how virtual contexts shape social presence, interpersonal dynamics, and collaboration [18, 63], explaining the emergence of group norms in digital spaces. MR adds further complexity by merging real and virtual worlds, introducing novel factors such as altered spatial awareness [37], shifts in presence [28], multimodal communication channels [62], and privacy concerns [53] that distinguish collaborative MR from traditional face-to-face interaction and fully immersive VR environments.

Despite this rich collaborative potential, most MR studies focus on individual user applications such as overlays for walking [34], biking [41] or driving [60, 55] rather than multiuser collaboration. Prior work in immersive environments has utilized multimodal sensors to capture group interactions, including sociometric badges for VR team cohesion analysis [75], gaze and controller motion for turn-taking characterization [9, 48], and head pose/gesture recording for task coordination [16]. However, these approaches are typically designed for offline or lab-based analysis rather than deployable, real-time sensing.

Building on established ubiquitous computing principles, prior research demonstrates that simple audio, location, and motion signals can reveal rich social dynamics [32, 50]. Social Network Analysis (SNA) and sociometry provide systematic frameworks for translating these behavioral signals into sociograms that visualize and quantify relationships, roles, and subgroup structures [46, 68]. This sensor-to-network approach has proven effective across domains, from nursing teams [12] to classroom groups [52], with recent work in virtual environments showing how gaze-based networks reveal patterns of leadership and cohesion [3, 71]. However, these approaches yield static, session-wide snapshots and require external hardware or manual annotation, leaving a gap in fully automated, real-time inference of moment-to-moment group behavior using only built-in MR headset sensors. While previous systems rely on dedicated hardware or fixed installations, **MURMR** brings on-device social signal processing to commodity MR headsets, computing sociometric indicators without additional instrumentation and enabling scalable deployment of adaptive collaborative MR applications.

However, these approaches yield static, session wide snapshots and require extra hardware or manual annotation, leaving a gap in fully automated, in-situ inference of moment-to-moment group behavior using only the sensors built into MR headsets. While previous systems rely on dedicated hardware or fixed installations, our framework **MURMR** brings on-device social signal processing to

MR headsets to compute sociometric indicators without extra instrumentation, enabling scalable deployment of collaborative MR applications that can adapt to group dynamics.

### 2.2 Mixed Reality Collaboration Frameworks

Research in Human-Computer Interaction (HCI) and immersive analytics has produced a range of systems for analyzing MR collaboration. Early empirical studies, such as Yang et al. [71], confirmed that immersive environments offer richer interaction than desktop setups, but relied on laborious manual coding of behaviors without automated or subgroup-level metrics.

A second wave introduced framework-style contributions for structured analysis. Systems such as Collaboration Translucence by Echeverria et al. [14] and ISA [35] enabled post-hoc visualization of multimodal logs through sociograms and timelines, although interpretation remained manual. Others focused on replay and reproducibility: PLUME [30] introduced standardized formats for single-user analytics, while ReLive [27] and MIRIA [7] supported session review for multi-user MR studies.

Finally, infrastructure toolkits like PSI [1] and MRAT [47] successfully lowered technical barriers to logging XR data but did not provide tools for inferring higher-order social dynamics. We summarize existing systems in Table 1, comparing eleven key dimensions including collaboration metrics, automated sociometric analysis, unsupervised inference capabilities, headset-only processing, real-time analysis, group-level support, subgroup detection, multiuser synchronization, replay environments, manual coding support, and open data formats for research reproducibility.

Although these systems provide foundational capabilities for replay and manual analysis, a critical gap remains as evidenced by Table 1. No prior system combines automated metrics, unsupervised inference, and headset-only sensing to analyze group-level social dynamics. Current tools largely depend on post-hoc manual interpretation and lack robust methods for unsupervised subgroup detection, limitations evident across all systems in our comparison.

**MURMR** addresses this gap by introducing a framework that transforms raw multimodal sensor data from MR headsets into higher-order sociometric constructs through automated network analysis and unsupervised temporal clustering. **MURMR** is the first system to deliver this combination of capabilities, eliminating the need for external hardware or manual annotation. While this study validates the core pipeline through offline evaluation, the modular architecture supports future real-time deployment, providing the foundation for adaptive collaborative MR systems with live sociometric feedback.

### 3 SYSTEM DESIGN AND IMPLEMENTATION

Analyzing group behavior in MR demands methods that preserve natural interaction while still producing timely, reliable insights. **MURMR** is designed to be an *in situ*, passive group behavior sensing framework in collaborative MR environments. Our framework addresses three key design principles: (1) synchronizing multimodal sensor data across multiple headsets without any external infrastructure by *multimodal sensor integration* (§3.1), (2) extracting rich, meaningful interaction features from commodity headset sensors using *sociogram-based structural analysis* (§3.2), and (3) identifying evolving phases of group behavior through *temporal clustering for dynamic pattern discovery* (§3.3).

We implement our modular framework as shown in Figure 1, **MURMR** captures and synchronizes multi-headset sensor data to maintain consistency between sensing modalities. This synchronized multimodal data stream is then fed into our two analysis modules: (1) Macro-level structural analysis module which extracts dyadic primitives (gaze, speech, proximity), and builds sociograms for role analysis, and (2) Micro-level temporal analysis module which segments various interactions into short-time windows for pattern identification. These two modules generate comprehensive post-session insights, including structural network metrics, temporal behavioral segmentation timelines, and dyadic interaction patterns that capture the various aspects of a collaborative group.

#### 3.1 Multi-Model Passive Sensing Module

**MURMR** exploits a full suite of built-in MR headset sensors. In particular, we are interested in observing information related to three types of interaction, namely conversation via audio, joint attention via gaze, and proximity via position data, as they have shown relevance to unraveling group behavior in various works in the literature [32, 50, 66, 73, 26, 11]. During each MR session, we collect the following data:

**Audio.** Ubiquitous sensor studies confirm that speech activities have long been shown to be critical for understanding small group interaction [50, 75], and their patterns shift across platforms from desktop to VR [71]. We track conversation via headset microphones and use Pyannote [6] for speaker diarization and voice activity detection, which timestamps each user’s speech segments and identifies speakers through acoustic feature clustering to capture verbal participation patterns.

**Gaze.** Building on extensive work in joint attention and gaze awareness for collaboration [66, 73], we capture joint attention from synchronized gaze rays whenever two users’ gaze vectors intersect the same virtual object or region.

**Position.** We capture physical proximity from six-degree-of-freedom (6DoF) headset poses (a proxy for social interaction [26, 11]) with spatial coordination recorded whenever participants remain within a close distance of one another.

To maintain consistency across sensing modalities, we perform post-session temporal synchronization by cross-referencing timestamps across all headsets to align coordinated behaviors such as joint attention and verbal participation with sub-100 ms precision using the network time protocol (NTP)-based clock alignment [45], since gaze convergence events occur within 50 ms-100 ms windows [70]. Our synchronization method addresses the multimodal nature of the data streams: audio data is captured at 44.1 kHz sampling rates with timestamps, then synchronized using the Pydub library for consistent temporal alignment across all participants. Spatial data synchronization uses shared spatial anchors via Photon Unity Networking to maintain a unified coordinate system across all MR headsets, with position data recorded at 1 Hz intervals. Eye-tracking data are timestamped at the sensor level and aligned with the shared temporal reference frame. To ensure data quality, we excluded the first 15 s of each session to remove noise from the application loading and initialization phases.

Together, these timestamped streams of audio, gaze, and position data from all headsets form the basis for both the macro-level, session-level, structured network analysis and the micro-level, fine-grained temporal clustering of dynamic group behavior. Passive data collection occurs entirely during the MR session, with post-hoc synchronization performed by cross-referencing timestamps across all four headsets. Processing and analysis are performed offline, enabling scalable deployment without impacting the *in situ* user experience.

#### 3.2 Structural Analysis Module

Sociograms, first popularized in social psychology to visualize group dynamics [46], are network representations that capture social relationships and interaction patterns in groups, providing a concise snapshot of who interacts with whom and how strongly. See Figure 1 for an example of a sociogram. In **MURMR**, we generate an automated sociogram, translating the synchronized sensor streams into a series of weighted interaction graphs, where each node is a *participant*, and the weight of each edge reflects the cumulative interaction strength across audio, gaze, and position modalities. This automated and annotation-free process produces static snapshots of the group structure, revealing emergent leaders, subgroup clusters, and overall cohesion as we will show in our evaluation in §5.1.

##### 3.2.1 Feature Selection

We focus on interaction channels from three main modalities.

First, *conversation patterns* serve as an insight into turn-taking dynamics and conversational balance. Beyond simply summing speaking time, we compute measures such as speaking-turn entropy (how evenly the conversation is shared) and overlap rate (frequency of interruptions or back-channels). These metrics map onto constructs of dominance and engagement established in small-group studies [57, 50]. Speech segments shorter than 0.5 s are discarded to filter out non-substantive utterances, while longer turns are attributed directionally to capture the speaker–listener asymmetry intrinsic to group dialogue.

Second, *joint attention* reflects the coordination of visual focus, which captures and underpins joint problem solving and mutual awareness. We detect joint fixations by intersecting each user’s 3D gaze vector with virtual objects and counting only overlaps that exceed fleeting glances. From these events, we set the edge weights to the total duration and fixation frequency, and mean inter-fixation interval, allowing us to distinguish sustained collaboration on a single artifact from rapid visual shifts across multiple items.

Third, *physical proximity* captures embodied aspects of collaboration that foster informal communication and trust [26, 67]. Using 6DoF head pose data, we record both the cumulative time dyads spend within a distance threshold and their approach-and-withdraw dynamics, quantified as the rate of change in inter-headset distance. These features differentiate static closeness, such as huddling around a shared task, from dynamic movement patterns that signal pacing, positional coordination, or coordinated repositioning.

We omit gesture and facial-expression cues, as capturing them reliably would require external cameras, which are incompatible with our design principles of untethered MR deployment.

##### 3.2.2 Modality-Specific and Fused Sociogram Construction

We construct a separate sociogram for each modality rather than scattering metrics across them. This is to isolate behaviors that could otherwise be conflated (for example, participants who remain physically close yet do not speak) and to maintain operational analysis when a sensor stream is temporarily unavailable. For each session, we generate a sociogram per interaction channel (conversation, joint attention, and proximity). We then merge the three

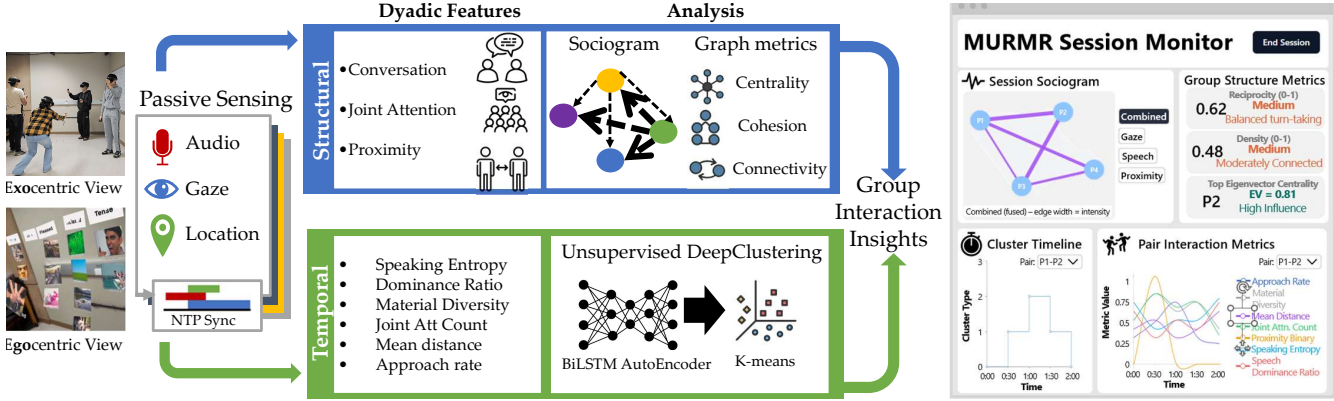


Figure 1: **MURMR** framework for sensing and analyzing collaborative group behavior in MR, starts by synchronizing multimodal sensor data to maintain consistency, then operates at two complementary modules. [Left] At a macro-level, session-long sensor data is aggregated to build sociograms that reveal overall group structure. At a micro-level, a temporal analysis of short interaction windows classifies fine-grained behavioral patterns. [Right] These analytics generate comprehensive post-session insights, including structural network metrics, temporal behavioral segmentation timelines, and dyadic interaction patterns that capture the various aspects of collaborative group behavior.

modality-specific sociograms into a *fused multimodal sociogram*, providing a comprehensive view of group interactions.

For accurate behavioral measurement, we apply empirically validated thresholds to filter noise from each sensor modality before constructing interaction graphs. For gaze tracking, overlaps between participants must persist for at least 13 ms, corresponding to the minimum visual processing latency required for joint attention detection [51]. Proximity interactions are recorded only when participants remain within 1.5 ft of each other, matching Hall’s intimate-distance zone [23]. Finally, conversational edges incorporate speech segments of 0.5 s or longer to preserve substantive utterances while filtering out breaths and back-channels [59]. These preprocessed, threshold-filtered data streams then serve as input for our sociogram construction:

- **Analysis Granularity.** We construct sociograms at two granularities: session-level aggregations capturing overall interaction patterns, and sliding 32 s windows with 16 s stride for dynamic analysis. The 32 s window duration provides sufficient interaction events to generate stable edge weights while remaining sensitive to behavioral transitions that typically occur on sub-minute timescales in collaborative tasks (parameter selection detailed in §3.3.4). The 16 s overlap between consecutive windows ensures continuity in tracking evolving group dynamics. This dual-granularity approach enables structural network analysis of both overall and moment-to-moment collaboration patterns.
- **Edge definition.** In each window, we assign edge weights based on the total *duration* of interaction. For conversation, the sum of spoken time; for joint attention, the overlap of gaze fixations; and for proximity, the accumulated intervals of co-presence within the defined distance threshold, as discussed before. Longer and sustained interactions, therefore, contribute more heavily than brief encounters. To capture directional dynamics, conversation graphs are treated as directed, reflecting the asymmetry between speaker and listener. Joint attention and proximity networks remain undirected, as these forms of engagement are inherently mutual.
- **Fused graph.** After constructing three separate sociograms represented in adjacency matrices, we normalize each adjacency matrix and fuse them into a single multimodal network using PCA-derived weights so that each channel contributes proportionally while retaining the directed nature of conversational ties (see §3.2.4).

### 3.2.3 Network Measures for Behavioral Insights

We use three primary network measures (centrality, cohesion, and connectivity) to analyze and interpret group behavior in mixed reality environments. These measures provide high-level insight into the dynamics of collaboration.

*Centrality measures* highlight participants who act as leaders or brokers within conversation and joint attention networks. *Cohesion measures* capture how tightly connected subgroups are, through physical proximity or mutual gaze. Finally, *connectivity* in the conversation graph is quantified via the reciprocity metric, which indicates the balance of two-way exchanges.

Together, these metrics provide both a static snapshot of the group structure and a means to track how roles, subgrouping, and engagement evolve over time. We summarize how each metric is mapped onto interpretable aspects of group behavior in Table 2. We compute these metrics on the directed conversation graphs and the undirected attention and proximity sociograms, and then we apply them to the fused multimodal sociogram to capture combined interaction effects.

To translate the constructed sociogram into interpretable group-level insights, we convert each of those network metrics into a three-tiered scale designed to capture behaviorally meaningful distinctions in collaborative patterns. For metrics with sufficient variance, we use session-relative percentiles with an emphasis on identifying outliers: **high** (*high*: top 16% of values (or  $z \geq +1$ ), **medium**: middle 68%, and **low**: bottom 16% (or  $z \leq -1$ )). This distribution prioritizes detection of extreme collaborative behaviors (highly central actors, isolated participants) while maintaining a substantial middle category for typical interaction patterns. While not intended as a rigid behavioral cutoff, the  $z$ -score with  $\pm 1$  rule provides a transparent and statistically grounded method for highlighting individuals who substantially exceed or fall below group norms.

### 3.2.4 Implementation Details

For each sliding window  $[t_0, t_1]$  applied to the time-series behavioral data stream—containing timestamped speech segments, gaze events, and headset position, we maintain three  $N \times N$  adjacency matrices  $W^{(\text{conv})}, W^{(\text{att})}, W^{(\text{prox})}$ , indexed by participant pairs.

In the **conversation** graph, we initialize  $W^{(\text{conv})} \leftarrow 0$  at the start of each window. For every speech segment  $(s_{\text{start}}, s_{\text{end}}, p)$  overlapping  $[t_0, t_1]$ , we compute  $\Delta = \min(s_{\text{end}}, t_1) - \max(s_{\text{start}}, t_0)$ .

Table 2: Interpretation of network metrics by interaction mode. Conv: conversation, Att: joint attention, Prox: proximity.

Modality	Metric (Ref.)	High Value Interpretation	Low Value Interpretation
<b>Centrality measures</b> identify potential leaders and information brokers in conversation and attention networks.			
Conv, Att, Prox	Eigenvector [17]	Connected to other highly central participants	Linked mainly to peripheral participants
<b>Cohesion measures</b> quantify bonding and tightness in proximity and attention networks.			
Att, Prox	Clustering Coef. [69]	High values indicate that a node's neighbors are densely interconnected, reflecting tight local subgroup cohesion	Low values indicate sparse neighbor connections, reflecting weak local cohesion
Conv, Att, Prox	Density [58]	High values signify a well-connected network with active group engagement	Low values signify a fragmented or minimally interacting group
<b>Connectivity measures</b> assess the balance of two-way exchanges in the conversation network.			
Conv	Reciprocity [24]	Balanced two-way exchanges (dialogue)	Predominantly one-way communication

If  $\Delta \geq 0.5$ , we capture the total time participant  $p$  spoke to every other member  $q$  as:  $W_{pq}^{(\text{conv})} += \Delta$

For **attention**, we clip each user's gaze intervals to the window  $[t_0, t_1]$  and, for each unordered pair  $(i, j)$ , sum all overlapping gaze durations  $\delta \geq 13$  ms, so that repeated joint fixations accumulate into a stronger undirected tie. We set:  $W_{ij}^{(\text{att})} = W_{ji}^{(\text{att})} = \sum \delta$

For **proximity**, we align headset poses at common timestamps in  $[t_0, t_1]$  and treat each inter-sample interval  $\Delta t$  as a unit of time. Whenever the pairwise distance  $d_{ij} \leq 1.5$  ft, we increment:

$$W_{ij}^{(\text{prox})} = W_{ji}^{(\text{prox})} + \Delta t$$

Finally, we fuse these three modality-specific matrices into a single multimodal *fused* adjacency matrix, where  $\{\alpha_m\}$  are principal component analysis (PCA) derived weights summing to 1 so that each channel contributes proportionally as:

$$W^{(\text{fused})} = \sum_{m \in \{\text{conv, att, prox}\}} \alpha_m W^{(m)}$$

All thresholds (0.5 s for speech, 13 ms for gaze overlap, 1.5 ft for proximity) are configurable, as are window length and stride. Each execution yields an instantaneous sociogram ready for metric computation or logging.

### 3.3 Temporal Analysis Module

Sociograms offer a static snapshot of group interactions over full sessions or windowed aggregates, but they can not detect when particular interaction patterns emerge or dissolve. Our temporal analysis addresses this by segmenting each session's dyadic behavioral features (such as balanced engagement, leader-driven dialogue or disengagement) into temporal phases via unsupervised clustering of time-series features.

#### 3.3.1 Feature Selection and Construction.

We standardize our initial pool of 24 dyadic behavioral features extracted from moment-to-moment participant interactions at one-second intervals. We then remove features with low variance, high pairwise correlation ( $r \geq 0.95$ ), or minimal impact on clustering quality, as determined by silhouette-based importance ranking. This pruning yields a concise feature representation spanning the following core behavioral dimensions:

**Verbal dynamics** are captured via *entropySpeaking* quantifying unpredictability in turn-taking, and *dominance\_ratio*, the imbalance in total speaking time per dyad.

**Interaction diversity** is measured with *material\_diversity*, which counts the distinct objects both participants jointly attend to, reflecting the richness of their shared focus.

**Proximity** is captured by features that characterize static closeness and dynamic movement patterns, *dist\_mean* is average dyadic distance, *prox\_binary* measures co-presence within 1.5ft, and *approach\_rate* to capture the speed of movement toward or away.

**Joint attention** (*joint\_att\_cnt*) counts the number of joint gaze fixations on the same virtual object, indicating peaks of mutual engagement.

All features are computed at one-second intervals,  $z$ -normalized per dyad, and aligned to a uniform temporal grid. This reduced feature set captures both transient and sustained collaboration signals, providing high-resolution temporal segmentation while remaining computationally minimal.

#### 3.3.2 Sequence Encoding and Model Architecture.

We treat each dyad's interaction over a segment as a  $T \times F$  matrix, where  $T$  is the number of 1s windows per segment and  $F = 7$  is the number of retained features. We determine both  $T$  and the stride  $S$  via grid search, optimizing for cluster coherence on held-out data; in practice, we use partial overlap ( $S < T$ ) to balance temporal resolution and embedding stability. Each sequence is processed by a deep clustering architecture: a convolutional-recurrent auto-encoder [38, 72] implemented in PyTorch. Two 1-D convolutional layers (with kernel sizes and filter counts selected via grid search) followed by ReLU activations and max-pooling extract local temporal patterns. A bidirectional LSTM then ingests the pooled features, producing a fixed-length latent vector. The decoder mirrors this architecture, upsampling and LSTM layers reconstruct the original sequence. Hyperparameters such as convolutional kernel dimensions, LSTM hidden state size, and dropout rate are tuned to maximize silhouette scores while maintaining low reconstruction error.

#### 3.3.3 Clustering and Loss Function.

The trained encoder maps each segment to a latent embedding, which we cluster using  $K$ -Means. To jointly optimize embeddings, both reconstruct their inputs accurately and form tight, well-separated clusters, we minimize the composite loss as:

$$\mathcal{L} = (1 - \lambda) \mathcal{L}_{\text{rec}} + \lambda \mathcal{L}_{\text{clu}} \quad (1)$$

$\mathcal{L}_{\text{rec}}$  is the mean squared reconstruction loss and  $\mathcal{L}_{\text{clu}}$  is the squared Euclidean distance to the assigned cluster centroid. We sweep cluster weight ( $\lambda$ ) in  $[0.3, 0.7]$ , choosing the value that yields the best trade-off between silhouette score and reconstruction fidelity. When the number of clusters  $k$  is unspecified, we apply a stability-informed elbow criterion, combining within-cluster inertia with cross-run adjusted Rand index (ARI) consistency to select  $k$ .

#### 3.3.4 Window Length and Stride Selection

To optimize clustering performance, we evaluate three  $\langle \text{window:stride} \rangle$  combinations ( $\langle 8:4 \rangle$ ,  $\langle 16:8 \rangle$  and  $\langle 32:16 \rangle$ ). Longer windows yielded slightly higher reconstruction error but notably better silhouette scores, improving progressively from 0.9247 (4s) to 0.9306 (32s), a 0.6% increase in cluster coherence. However, performance gains plateaued

beyond 16s, with only a 0.2% improvement from 16s to 32s (0.0014 increase) compared to 0.3% from 8s to 16s (0.0025 increase). Increasing the stride to 16s further improved cluster separation by 0.2% over 8s stride (0.9308 vs 0.9285), with only a marginal impact on loss. We therefore use a 32s window and 16s stride throughout, which also aligns our temporal clusters with the sociogram snapshots and ensures at least 30s of data per network for stable metric estimation.

### 3.3.5 Implementation and Output.

All heavy computations, such as feature extraction, encoding, and clustering, are performed offline after data collection. To scale across many dyads or lengthy sessions, these tasks run in parallel, and a *fast evaluation mode* subsamples up to 5000 windows, cutting runtime from  $\approx 30$  min to under 5 min with negligible quality loss. While offline training requires significant resources, real-time deployment would only require inference on pre-trained models for individual 32-second windows, substantially reducing computational overhead. The module outputs a cluster label for each dyadic window, which can be rendered as phase-aligned timelines or heatmaps, offering a time-resolved map of how group behavioral patterns evolve. More details will be discussed in the evaluation in §5.2

## 3.4 MURMR Analytics Dashboard

The two modules in **MURMR** generate comprehensive analytical outputs that translate raw sensor data into actionable collaboration insights. Figure 1 illustrates how these analytics are structured in three complementary analytical perspectives that provide researchers and facilitators with an understanding of group dynamics.

- *Structural Network Analysis Results:* The PCA-fused sociograms reveal overall group cohesion patterns and interaction hierarchies throughout the entire session. Session-wide metrics, including reciprocity, density, and eigenvector centrality, quantify the group’s collaborative structure, identifying emergent leaders, balanced versus hierarchical communication patterns, and overall engagement levels. The modality-specific sociograms (conversation, gaze, proximity) isolate distinct behavioral channels, revealing whether groups coordinate primarily through physical proximity, shared visual attention, or verbal communication.
- *Temporal Behavioral Segmentation:* Our unsupervised clustering identifies distinct phases of collaborative behavior, segmenting sessions into interpretable behavioral patterns. This temporal analysis reveals the sequence and duration of different collaborative states, showing how groups transition between focused work periods, active discussion phases, and leadership-driven instruction moments.
- *Dyadic Interaction Dynamics:* The pairwise analysis exposes the micro-dynamics of collaboration, tracking how specific partnerships contribute to overall group performance. By analyzing individual dyads’ interaction patterns over time, researchers can identify which pairs drive collaborative transitions, maintain group cohesion during difficult phases, or create bottlenecks in information flow.

These complementary analyses provide a holistic picture of collaboration. Structural metrics reveal “who collaborates with whom,” temporal clustering shows “when different collaboration modes occur,” and dyadic analysis explains “how specific relationships shape group dynamics.” This multi-perspective approach addresses the critical gap in collaboration research by capturing both static interaction patterns and dynamic behavioral evolution throughout MR sessions.

## 4 DEPLOYMENT AND STUDY SETUP

### 4.1 Participants

We recruited 48 participants (12 groups of 4; 36 male, 8 female; age mean ( $\mu$ ) = 24.2, standard deviation (SD) = 4.7). Pre-study demographic questionnaires measured prior immersive-tech experience on 7-point Likert scales: MR ( $\mu = 1.8, SD = 1.2$ ), AR ( $\mu = 3.1, SD = 1.8$ ), VR ( $\mu = 3.4, SD = 2.1$ ). We fixed the group size at four to maximize the number of dyadic interactions (six per group) while keeping computation tractable [65].

### 4.2 Materials

We conducted the study in 10 ft  $\times$  5 ft space where participants navigated and collaborated in close quarters (cleared of materials to minimize distractions). Each participant used a Meta Quest Pro headset [44], which captured and streamed eye gaze, binaural audio, and 6DoF pose data over our local Wi-Fi network. We synchronized all devices with NTP (<50 ms offset) and built the collaborative MR app in Unity with the Meta XR SDK [43]. We aligned every virtual object in each user’s coordinate frame so that there was a shared reference without any additional prompts, cues, or enforced turn-taking.

### 4.3 Collaborative Task

We asked each group to sort the 28 OASIS images [33] (validated for pleasantness and arousal and free of graphic content) into six affective labels (angry, bored, relaxed, tense, pleased, frustrated) based on Russell’s circumplex model [56]. The virtual images were scattered throughout, overlayed on the see-through physical space, with floating *plates* labeled for each emotion hovering nearby. Without any time limit or scripted turns, participants freely approached and grabbed images, moved them to their chosen plates, and negotiated assignments through open-ended discussion. To sort an image, participants used a natural point-and-drag motion with their Meta Quest Pro controllers. They aimed at an image, held the grip button to *pick it up*, guided it toward the desired emotion plate, and released the button to lock it in place. Images only attach when positioned sufficiently close to a label, providing immediate visual confirmation. Only one person can manipulate a given image at a time, but different participants may simultaneously move other images within reach, mirroring the physical act of picking up and placing objects. This unstructured setting, where teams self-direct by clustering around images of interest, encourages natural decision-making, communication, and alignment as group members iteratively build consensus on each label [54, 5, 4]. On average, the groups completed the task in 32.4 minutes (SD = 8.4).

### 4.4 Procedure

Upon arrival, participants reviewed an IRB-approved information sheet and provided verbal consent, then completed a brief demographics survey. We handed out Meta Quest Pro headsets, guided each person through focus and fit calibration, and ran a short tutorial using two practice images and categories to teach the grab–drag–release interaction and category placement in MR. Next, groups tackled the main task, sorting 28 images into 6 emotion categories. We instructed them to *work together to categorize these images by emotion, discuss and reach agreement on each label*, with no time limit or performance feedback. Participants self-directed their collaboration, moving freely around the space and negotiating assignments until everyone confirmed consensus. After they finished sorting, the session concluded, and participants returned their headsets. The entire session, including setup, training, task, and wrap-up, took under 35 – 45 minutes.

### 4.5 Data Collection and Ground Truth

We captured multimodal data passively from each headset with post-hoc synchronization and ran it through **MURMR**’s end-to-end

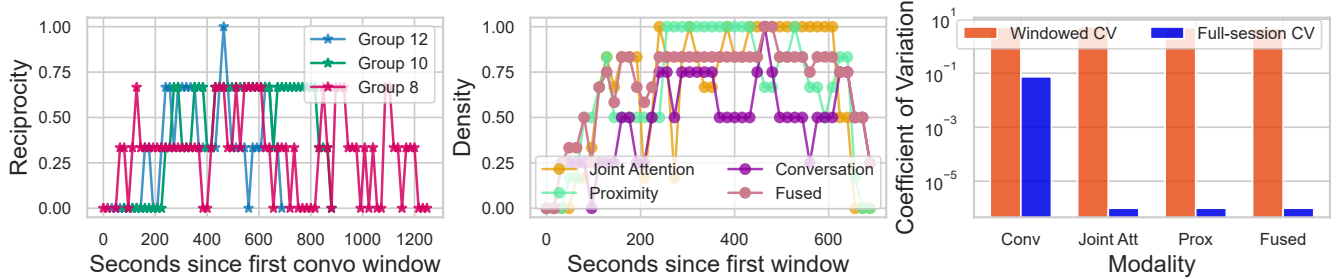


Figure 2: Windowed-session analysis to assess behavioral patterns obscured by session-level aggregation. Conversation reciprocity for representative Groups 8, 10, 12 (left), Group 12’s multimodal density trajectory (center), and density variation (right).

pipeline to analyze group behavior. To validate these automated inferences, we first assessed clustering stability and checked that sociogram metrics remained consistent across time and groups. *We deliberately omitted subjective collaboration surveys; such ratings cannot reliably capture the dynamic, moment-to-moment shifts our system targets [10] and would not align with its end-to-end, automated design.* Therefore, we manually validated our results against time-aligned passively collected egocentric video from each headset, confirming the system corresponded to actual behaviors on camera; this served as our ground truth <sup>1</sup> This multi-layered validation cluster stability, consistent sociogram metrics, human annotation with egocentric videos demonstrates **MURMR**’s robustness and scalability for passive, real-world MR group settings.

#### 4.6 Real-time Deployment Prototype

**MURMR**’s architecture supports future real-time deployment through multimodal data streaming from four concurrent Meta Quest Pro headsets. Real-time streaming maintained 70 – 72 FPS while capturing multimodal data streams (audio, gaze, spatial, gestural) via standard TCP/IP over consumer WiFi hardware. While our study used offline analysis, the system’s 32 s analysis windows and demonstrated streaming performance establish technical feasibility for live behavioral classification. Streaming validation confirmed deployment readiness: 1% battery consumption per minute supports 90-minute sessions, dynamic buffer scaling handles peak data loads, and consumer-grade networking eliminates specialized infrastructure requirements.

## 5 RESULTS

### 5.1 Structural Analysis of Group Behavior

To understand how collaboration evolves, we contrasted static, session-long interaction patterns with a dynamic, moment-to-moment analysis. The static view, aggregating all of the interaction within a session, presented a deceptively stable picture, with minimal variation across modalities presented as coefficient of variation ( $CV$  : 0.000 – 0.074). In stark contrast, 32 s sliding window analysis revealed the true, fluctuating nature of teamwork, exposing significant variability in interaction structures ( $CV$  : 4.626 – 5.261), as visualized in Figure 2 (right panel), which uses a logarithmic y-axis to display the stark contrast between the two analytical approaches effectively. This demonstrates that analyzing an entire session in aggregate obscures critical episodes of intense collaboration, subgroup formation, and shifting interaction patterns that define the collaborative process.

To further illustrate the diverse collaborative dynamics uncovered by our structural analysis, we selected three exemplar groups

<sup>1</sup>Our framework **MURMR** is fully automated without the need for egocentric videos for group behavior analysis. However, these videos were collected only to validate the framework as the ground truth.

Table 3: Group screening metrics: change and variance reciprocity as well as mean fused density for each of the 12 groups.

Group	$\Delta$ Reciprocity	$\sigma$ Reciprocity	Fused Density
1.0	1.0	0.085	0.005
2.0	0.667	0.055	0.005
3.0	0.667	0.064	0.609
4.0	0.667	0.047	0.122
5.0	0.333	0.029	0.372
6.0	1.0	0.079	0.612
7.0	1.0	0.132	0.734
8.0	0.667	0.054	0.716
9.0	1.0	0.058	0.673
10.0	0.667	0.075	0.723
11.0	1.0	0.152	0.684
12.0	1.0	0.072	0.688

(Figure 2, left panel). These groups show different profiles of reciprocity. Group 8 ( $\mu = 0.308, \sigma = 0.233$ ) exemplifies a pattern of less reciprocity, suggesting a more hierarchical or fragmented interaction style where communication was often one-directional. In contrast, Group 10 ( $\mu = 0.451, \sigma = 0.273$ ) demonstrated a more balanced and collaborative pattern with frequent mutual exchanges. Group 12 ( $\mu = 0.350, \sigma = 0.268$ ) represents a highly variable dynamic; its ability to achieve moments of perfect reciprocity ( $range : 0.0 – 1.0$ ) was a pattern observed across the majority of teams (7 of 12 groups) as seen in Table 3, indicating that groups fluidly transitioned between fractured and highly synchronized interaction states.

Our multimodal fusion analysis, which combines behavioral cues into a single measure of interaction strength, revealed that collaboration was overwhelmingly defined by physical and visual co-presence. Proximity (loading = 0.631,  $\sigma = 0.061$ ) and joint attention (loading = 0.637,  $\sigma = 0.054$ ) were the dominant components, indicating that being near a partner and looking at the same object were the primary drivers of dyadic connection. Conversely, conversation showed a minimal and highly variable structural contribution (loading = -0.088,  $\sigma = 0.446$ ). This is clearly visible in Group 12’s data (Figure 2, center panel), where the fused interaction density closely mirrors the trajectories of proximity and joint attention, not conversation.

To assess each modality’s contribution to our PCA-based multimodal fusion, we conducted leave-one-out ablation. For each condition, we excluded one modality (conversation, joint attention, or proximity) from the PCA weight calculation process and recomputed fusion weights using only the remaining two modalities. We then reconstructed the fused sociograms and measured how well the original dyadic edge weight rankings were preserved using Spearman correlation ( $\rho$ ) between the complete three-modality fusion

and each two-modality ablated version. This approach isolates each modality’s structural contribution to the final interaction representation without requiring clustering model retraining. Results confirmed proximity’s foundational role: removing it fundamentally disrupted the dyadic rankings ( $\rho = -0.26, p = 0.62$ ). Removing conversation ( $\rho = 0.94, p < 0.001$ ) left the core interaction structure nearly perfectly intact, while removing joint attention showed a moderate impact ( $\rho = 0.77, p < 0.07$ ). These findings verify that proximity serves as the structural backbone of our fusion model, with joint attention providing meaningful but secondary contributions, and conversational patterns being largely redundant with the spatial-visual interaction framework.

Together, these findings establish that a granular, windowed analysis is essential for capturing interaction dynamics that are invisible in session-level aggregation. Our results indicate a clear division of labor among behavioral cues: proximity and joint attention define the structure of collaboration, determining who works with whom on a moment-to-moment basis. Conversation, in contrast, appears largely redundant with spatial-visual cues, contributing minimal additional structural information. Based on this, we recommend prioritizing proximity and joint attention in PCA-fused graphs for both real-time monitoring of group cohesion and post-hoc analysis of collaborative dynamics, as these modalities capture the essential structural backbone of teamwork.

## 5.2 Temporal Clustering of Dyadic Interactions

To capture how interaction dynamics evolve, we evaluate the behavioral patterns uncovered by our temporal clustering module.

### 5.2.1 Latent Embedding and Cluster Selection

We divided each session into 32s windows with a 16s stride, yielding 71404 dyadic segments. Each segment was encoded by a three-layer convolutional-recurrent autoencoder (latent dimension = 16). We then applied  $K$ -means ( $k = 2 - 10, 20$  restarts) to the learned embeddings. An inertia elbow, a silhouette score of 0.87, and an  $ARI > 0.8$  all pointed to  $k = 4$  clusters. The 16-dimensional embeddings are projected into 3D by UMAP in Figure 3, revealing four distinct clusters. The relative sizes of the clusters: 44.7%, 34.0%, 15.4%, and 5.8% for clusters 0, 1, 2, 3.

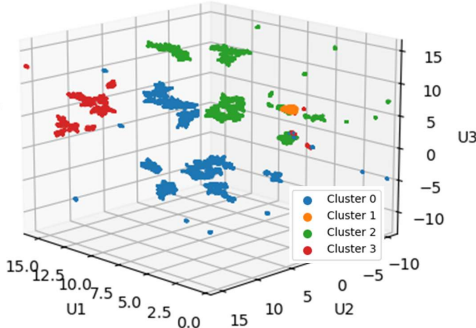


Figure 3: 3D UMAP of 71404 window embeddings. Colors denote clusters; distinct manifolds confirm high silhouette quality.

### 5.2.2 Cluster Characterization

We link each cluster to a distinct behavioral pattern by inspecting its  $z$ -scored feature profile (Figure 4). Cluster 0 shows high *dominance\_ratio*, low *speaking\_entropy*, and minimal proximity, indicative of structured, turn-based leadership with predictable dialogue pacing. Cluster 1 combines elevated *speaking\_entropy*, frequent *joint\_att\_cnt* events, and close proximity to capture animated, synchronous co-manipulation

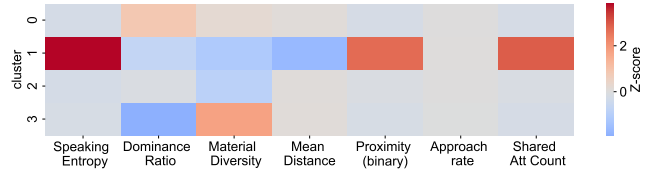


Figure 4: Heatmap of clusters (rows) vs. features (columns), where color intensity shows each feature’s deviation from its mean.

Table 4: Entropy of cluster membership across groups, pairs, and actors (lower values = more context-specific).

Cluster	Group Ent.	Pair Ent.	Actor Ent.
0 (Rhythmic Leader–Follower)	<b>1.23</b>	2.91	2.42
1 (Animated Collaboration)	2.47	3.41	2.85
2 (Monotone Focus)	2.10	2.68	2.21
3 (Instructor Demonstration)	2.60	<b>3.73</b>	2.88

marked by rapid speech and movement fluctuations. Cluster 2 features low *material\_diversity* and muted speech dynamics, reflecting a narrow, repetitive task focus with balanced but monotone interaction. Finally, Cluster 3 pairs high *material\_diversity* with low *dominance\_ratio*, embodying instructor-style demonstrations in which one participant explores varied content while others observe. Our clusters’ relative sizes as denoted in §5.2.1 indicate the rarity of instructor demonstration, with rhythmic leadership and monotone focus being more common.

### 5.2.3 Generalizability Across Dyads

We further validated our rule hierarchy using Shapley additive explanations (SHAP) values [36], which quantify each feature’s contribution to individual cluster predictions. We distilled each behavioral pattern into a clear decision hierarchy using a surrogate decision tree, with SHAP values confirming the relative importance of each feature. In practice, any 32s window with *speaking\_entropy*  $> 1.2$  is labeled as Cluster 1 (animated collaboration); if not, a *dominance\_ratio*  $< -0.7$  assigns it to Cluster 3 (instructor demonstration behavior); failing that, *material\_diversity*  $< -0.3$  indicates Cluster 2 (monotone focus); all remaining segments fall into Cluster 0 (rhythmic leadership). This sequence prioritizes conversational unpredictability first, then leadership asymmetry, and finally task variety.

To understand how these patterns distribute across teams and individuals, we computed the categorical entropy of cluster membership at the group, pair, and actor levels in Table 4. A low entropy score signifies a behavior that is tightly tied to specific contexts, while a high score points to a widely shared interaction style. Cluster 0 shows the lowest group entropy (1.23), indicating that rhythmic leader–follower patterns tend to be team-specific. By contrast, Cluster 1’s high entropy across all three levels confirms that animated collaboration is a universally occurring pattern. Clusters 2 and 3 occupy intermediate positions, revealing a blend of context-sensitive and broadly shared behaviors. These findings demonstrate that our temporal clustering identifies distinct interaction phases and captures their generalizability across diverse MR group settings.

**Manual Validation:** To assess the patterns revealed in clustering against human judgment, we randomly sampled 100 windows (evenly across the four predicted clusters, and balanced by group) to match available coding resources. Overall, human annotated labels agreed with our automated assignments in 71 cases (71% accuracy). Performance was consistent for Clusters 0–2. Precision

Table 5: Structural metrics whose low/medium/high tertile distributions show association with behavioral clusters ( $N = 11770$  windows).

Metric (binned)	$\chi^2$	$p$	Cramér’s $V$
Proximity Eigenvector	21.59	0.001	0.28
Conversation Eigenvector	16.49	0.011	0.24
Joint Attention Eigenvector	15.66	0.016	0.24
Fused Eigenvector	14.82	0.022	0.23
Conversation Reciprocity	12.67	0.049	0.41

ranged from 0.75 to 0.84, recall from 0.64 to 0.73, and  $F1 \approx 0.72$ . In contrast, Cluster 3 (instructor demonstration) achieved high recall (0.92) but lower precision (0.48), indicating that the model often over-predicted this state. Most misclassifications involved false positives for Cluster 3 or confusion between Clusters 0 and 2, whose feature profiles overlap partially. The macro-averaged metrics precision 0.71, recall 0.74, and  $F1 \approx 0.70$  confirm broadly uniform performance across clusters. These results suggest that the temporal analysis module reliably identifies the three dominant collaboration modes, while further refinement is needed to reduce false positives before using instructor demonstration labels for real-time adaptation.

### 5.3 Structural vs. Temporal Alignment

#### 5.3.1 Alignment of Clusters and Network Metrics

To verify that temporal and structural analyses capture similar collaborative behavior, we cross-tabulated the four behavioral clusters against tertile-binned network metrics across all analysis windows. After confirming chi-square ( $\chi^2$ ) assumptions, five metrics demonstrated significant associations with cluster membership (Table 5). Proximity eigenvector centrality exhibited the strongest relationship ( $\chi^2 = 21.59, p = 0.001, \text{Cramér’s } V = 0.28$ ), followed by conversation eigenvector centrality ( $\chi^2 = 16.49, p = 0.011, V = 0.24$ ), joint attention eigenvector centrality ( $\chi^2 = 15.66, p = 0.016, V = 0.24$ ), fused eigenvector centrality ( $\chi^2 = 14.82, p = 0.022, V = 0.23$ ), and conversation reciprocity ( $\chi^2 = 12.67, p = 0.049, V = 0.41$ ). Examination of contingency tables revealed that animated collaboration (Cluster 1) and instructor demonstration (Cluster 3) were predominantly represented in high-centrality tertiles across all network types. Notably, basic structural measures, including density and average clustering coefficient, were excluded from analysis because their values collapsed to single bins, indicating insufficient variation across behavioral clusters. This finding suggests that centrality-based metrics provide superior sensitivity to change the behavioral cluster labels transitions compared to global network properties.

#### 5.3.2 Illustrative Case Study: Lead–Lag Dynamics

To illustrate MURMR’s ability to capture lead–lag dynamics, Figure 5 plots the fused eigenvector trajectory for an illustrative dyad from Group 10. Over the 688 s session, the dyad alternates between an instructor demonstration mode (Cluster 3) and an animated collaboration mode (Cluster 1), with eigenvector centrality spanning from a minimum of 0.010 to a maximum of 0.500. A key transition from Cluster 3 to Cluster 1 occurs at 6 : 56, during a period when centrality is already sustained near its session maximum ( $EV \approx 0.495$ ). The dyad then remains in Cluster 1 for 32 s, with centrality holding stable within a high-value plateau ( $\mu EV \approx 0.491$ ). Subsequent returns to Cluster 3 (e.g., at 7:28 and 8:48) also occur while centrality is at its peak ( $EV \approx 0.500$ ). Notably, the average change in centrality across these transitions is minimal ( $avg|\Delta EV| \approx 0.003$ ), indicating that abrupt fluctuations in influence do not mark these shifts in interactional style. Rather,

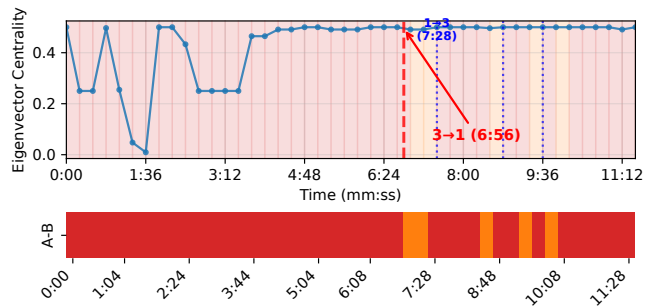


Figure 5: Fused eigenvector over time for one pair in Group 10, with the transition from Cluster 3 to Cluster 1 highlighted.

they represent changes in collaborative mode that take place within an established, stable state of high reciprocal influence.

## 6 DISCUSSION

Our temporal analysis reveals fundamental limitations in static methodologies for collaboration frameworks. While session-long analyses show stability, moment-to-moment examination exposes the dynamic processes that define collaboration: role negotiation, leadership shifts, and subgroup formation. Traditional static approaches systematically obscure these critical behaviors. MURMR’s methodological contribution captures collaboration’s inherently temporal nature, advancing the field beyond static analytical frameworks toward dynamic understanding of collaborative processes.

The hierarchy between proximity and conversation cues has important methodological implications. Our findings establish a functional division: proximity provides structural insights while conversation reveals content-level dynamics. This separation suggests that collaboration research should decouple structural monitoring from content analysis, enabling both real-time group tracking and detailed behavioral understanding. This methodological framework addresses current limitations in unified social sensing approaches.

Our automated clustering of collaborative patterns demonstrates that complex social dynamics can be reliably detected from sensor data. This capability enables large-scale analysis of collaborative processes, revealing both universal interaction patterns and context-specific adaptations. The automated detection of behavioral phases represents a significant advance toward adaptive systems that can respond to collaborative dynamics in real time, bridging the gap between collaboration research and practical applications.

Network structure serves as a leading indicator for collaborative transitions. Elevated reciprocity and centrality precede coordination phases, while conventional metrics miss these shifts. This predictive capability enables adaptive systems to anticipate group needs and provide timely interventions. These findings extend collaboration research toward real-time applications, establishing foundations for responsive collaborative environments that adapt to group dynamics.

### 6.1 Implications & Practical Recommendations

Our findings demonstrate that temporal analysis is essential for understanding collaboration’s episodic nature. The separation of proximity-driven structural analysis from conversational content analysis enables comprehensive interaction understanding. This methodological approach has direct practical applications: structural monitoring can serve as real-time group cohesion assessment, automatically detecting when teams become spatially fragmented and enabling timely interventions to maintain group coherence.

Automated classification of collaborative behaviors enables multiple practical applications. Real-time detection can identify prob-

lematic patterns—such as conversational imbalance or reduced engagement—allowing for immediate interventions. For practitioners, this technology offers objective assessment tools: facilitators gain data-driven insights for leadership development, while teams receive personalized coaching based on their specific interaction patterns. System designers can leverage these capabilities by implementing real-time adaptation mechanisms for immediate support and post-session analysis tools for reflective team development.

## 6.2 Limitations and Future Work

Our findings are based on one collaborative task with student groups in a controlled lab setting. The dominance of proximity as a structural driver may be specific to this co-located, object-focused context. Future work should validate **MURMR** longitudinally with in real-world settings to determine how interaction patterns generalize across different tasks, team structures, and timescales.

Our analytical approach has clear boundaries. Our threshold selections (gaze duration, proximity distance, and speech segment length) were chosen based on established research; however, they need a systematic sensitivity analysis across diverse MR collaboration scenarios, which could inform more robust parameter selection in future work. The 71% pattern classification accuracy relies on subjective, human annotated ground truth and simple decision-tree modeling. Future work should improve label robustness through interrater reliability analysis and explore other temporal models (LSTMs) to capture complex interaction dependencies. Furthermore, our system measures behavioral proxies rather than internal cognitive states. Integrating lightweight sentiment analysis or physiological sensors could provide richer, more direct collaborative measures.

Finally, **MURMR** currently demonstrates offline analysis, but the ultimate goal is real-time intervention through our conceptual dashboard. This requires engineering the analytics module for live computation to power real-time features and validating the dashboard’s real-world utility once functional. Our real-time streaming capability prototype provides the foundation for future adaptive collaboration systems that can deliver real-time feedback and intervention based on automatically detected group dynamics, addressing current limitations in collaborative MR research that rely on post-hoc analysis.

Our work infers social constructs, such as leadership, from behavioral proxies without validating these against participants’ subjective experiences. This prevents definitively linking detected patterns, like speech asymmetry, to perceived social realities like leadership. Our manual coding validates that behavioral patterns exist, but not their meaning to participants.

## 7 CONCLUSION

**MURMR** introduces a comprehensive platform for passive group behavior sensing in MR environments through complementary structural and temporal analysis modules. Our structural analysis module captures group organization through automated sociograms and reveals substantial behavioral variability across granular sliding windows that traditional session-level methods miss entirely. Our temporal analysis module performs unsupervised clustering to identify moment-to-moment dyadic interaction patterns between team members. Through 48-participant validation, we establish that multimodal analysis prioritizes proximity and joint attention for structural understanding, enabling lightweight monitoring approaches for real-time applications. These findings advance collaboration research by demonstrating that group-level structural dynamics and dyadic interaction patterns require distinct analytical approaches. This dual-module architecture provides methodological advancements for MR collaborative research and establishes foundations for adaptive applications that respond to both organizational and interpersonal dynamics.

## ACKNOWLEDGMENTS

This work is supported by the U.S. National Science Foundation (NSF) under grant number 2339266 and 2237485.

## REFERENCES

- [1] S. Andrist, D. Bohus, Z. Li, and M. Soleymani. Platform for situated intelligence and openseNSE: A tutorial on building multimodal interactive applications for research. In *Companion Publication of the 25th International Conference on Multimodal Interaction*, pp. 105–106, 2023. 2
- [2] H. Bai, P. Sasikumar, J. Yang, and M. Billinghurst. A user study on mixed reality remote collaboration with eye gaze and hand gesture sharing. In *Proceedings of the 2020 CHI conference on human factors in computing systems*, pp. 1–13, 2020. 1
- [3] J. N. Bailenson, A. C. Beall, J. Loomis, J. Blascovich, and M. Turk. Transformed social interaction: Decoupling representation from behavior and form in collaborative virtual environments. *Presence: Teleoperators & Virtual Environments*, 13(4):428–441, 2004. 2
- [4] N. Berlin, M. Gueye, and S. Monjon. Feedback and cooperation: An experiment in sorting behavior, 2025. 6
- [5] M. F. Bjerre. Card sorting as collaborative method for user-driven information organizing on a website: Recommendations for running collaborative group card sorts in practice. *Communication & Language at Work*, 4(4):74–87, 2015. 6
- [6] H. Bredin, R. Yin, J. M. Coria, G. Gelly, P. Korshunov, M. Lavechin, D. Fustes, H. Titeux, W. Bouaziz, and M.-P. Gill. Pyannote: audio: neural building blocks for speaker diarization. In *ICASSP 2020-2020 IEEE International Conference on Acoustics, Speech and Signal Processing (ICASSP)*, pp. 7124–7128. IEEE, 2020. 3
- [7] W. Büschel, A. Lehmann, and R. Dachselt. Miria: A mixed reality toolkit for the in-situ visualization and analysis of spatio-temporal interaction data. In *Proceedings of the 2021 CHI conference on human factors in computing systems*, pp. 1–15, 2021. 2
- [8] G. Cascini, J. O’Hare, E. Dekoninck, N. Becattini, J.-F. Boujut, F. B. Guefrache, I. Carli, G. Caruso, L. Giunta, and F. Morosi. Exploring the use of ar technology for co-creative product and packaging design. *Computers in Industry*, 123:103308, 2020. 1
- [9] D. Chaffin, R. Heidl, J. R. Hollenbeck, M. Howe, A. Yu, C. Voorhees, and R. Calantone. The promise and perils of wearable sensors in organizational research. *Organizational Research Methods*, 20(1):3–31, 2017. 2
- [10] Y. Chandio, V. Interrante, and F. M. Anwar. Reaction time as a proxy for presence in mixed reality with distraction. *IEEE Transactions on Visualization and Computer Graphics*, 2025. 7
- [11] M. Cristani, G. Paganetti, A. Vinciarelli, L. Bazzani, G. Menegaz, and V. Murino. Towards computational proxemics: Inferring social relations from interpersonal distances. In *2011 IEEE Third International Conference on Privacy, Security, Risk and Trust and 2011 IEEE Third International Conference on Social Computing*, pp. 290–297. IEEE, 2011. 3
- [12] A. Drahota and A. Dewey. The sociogram: A useful tool in the analysis of focus groups. *Nursing research*, 57(4):293–297, 2008. 2
- [13] J. Du, Y. Shi, C. Mei, J. Quarles, and W. Yan. Communication by interaction: A multiplayer vr environment for building walkthroughs. In *Construction Research Congress 2016*, pp. 2281–2290, 2016. 1
- [14] V. Echeverria, R. Martinez-Maldonado, and S. Buckingham Shum. Towards collaboration translucence: Giving meaning to multimodal group data. In *Proceedings of the 2019 chi conference on human factors in computing systems*, pp. 1–16, 2019. 2
- [15] S. Elmaliaki. Fair-iot: Fairness-aware human-in-the-loop reinforcement learning for harnessing human variability in personalized iot. In *Proceedings of the International Conference on Internet-of-Things Design and Implementation*, pp. 119–132, 2021. 1
- [16] B. Ens, J. Lanir, A. Tang, S. Bateman, G. Lee, T. Piumsomboon, and M. Billinghurst. Revisiting collaboration through mixed reality: The evolution of groupware. *International Journal of Human-Computer Studies*, 131:81–98, 2019. 1, 2

- [17] L. C. Freeman, D. Roeder, and R. R. Mulholland. Centrality in social networks: II. experimental results. *Social networks*, 2(2):119–141, 1979. 5
- [18] D. Gatica-Perez, L. McCowan, D. Zhang, and S. Bengio. Detecting group interest-level in meetings. In *Proceedings.(ICASSP'05). IEEE International Conference on Acoustics, Speech, and Signal Processing, 2005.*, vol. 1, pp. I–489. IEEE, 2005. 2
- [19] H. Gençer. Group dynamics and behaviour. *Universal Journal of Educational Research*, 2019. 1
- [20] J. Gerup, C. B. Soerensen, and P. Dieckmann. Augmented reality and mixed reality for healthcare education beyond surgery: an integrative review. 11:1–18, Jan. 2020. 1
- [21] M. Gonzalez-Franco, R. Pizarro, J. Cermeron, K. Li, J. Thorn, W. Hutabarat, A. Tiwari, and P. Bermell-Garcia. Immersive Mixed Reality for Manufacturing Training. *Frontiers in Robotics and AI*, 4, Feb. 2017. Publisher: Frontiers. 1
- [22] T. Halfhill, E. Sundstrom, J. Lahner, W. Calderone, and T. M. Nielsen. Group personality composition and group effectiveness: An integrative review of empirical research. *Small group research*, 36(1):83–105, 2005. 1
- [23] E. T. Hall, R. L. Birdwhistell, B. Bock, P. Bohannan, A. R. Diebold Jr, M. Durbin, M. S. Edmonson, J. Fischer, D. Hymes, S. T. Kimball, et al. Proxemics [and comments and replies]. *Current anthropology*, 9(2/3):83–108, 1968. 4
- [24] R. A. Hanneman and M. Riddle. Introduction to social network methods, 2005. 5
- [25] M. Higgs, U. Plewnia, and J. Ploch. Influence of team composition and task complexity on team performance. *Team Performance Management: An International Journal*, 11(7/8):227–250, 2005. 1
- [26] M. Hoegl and L. Proserpio. Team member proximity and teamwork in innovative projects. *Research Policy*, 33(8):1153–1165, Oct. 2004. 3
- [27] S. Hubenschmid, J. Wieland, D. I. Fink, A. Batch, J. Zagermann, N. Elmquist, and H. Reiterer. Relive: Bridging in-situ and ex-situ visual analytics for analyzing mixed reality user studies. In *Proceedings of the 2022 CHI Conference on Human Factors in Computing Systems*, pp. 1–20, 2022. 2
- [28] A. Irlitti, M. Latifoglu, Q. Zhou, M. N. Reinoso, T. Hoang, E. Veloso, and F. Vetro. Volumetric mixed reality telepresence for real-time cross modality collaboration. In *Proceedings of the 2023 CHI Conference on Human Factors in Computing Systems*, pp. 1–14, 2023. 1, 2
- [29] P. Jansen, J. Britten, A. Häusele, T. Segschneider, M. Colley, and E. Rukzio. Autovis: Enabling mixed-immersive analysis of automotive user interface interaction studies. In *Proceedings of the 2023 CHI conference on human factors in computing systems*, pp. 1–23, 2023. 2
- [30] C. Javerliat, S. Villenave, P. Raimbaud, and G. Lavoué. Plume: Record, replay, analyze and share user behavior in 6dof xr experiences. *IEEE Transactions on Visualization and Computer Graphics*, 30(5):2087–2097, 2024. 2
- [31] N. L. Kerr and R. S. Tindale. Group performance and decision making. *Annu. Rev. Psychol.*, 55(1):623–655, 2004. 1
- [32] T. Kim, E. McFee, D. O. Olguin, B. Waber, and A. Pentland. Sociometric badges: Using sensor technology to capture new forms of collaboration. *Journal of Organizational Behavior*, 33(3):412–427, 2012. 1, 2, 3
- [33] B. Kurdi, S. Lozano, and M. R. Banaji. Introducing the open affective standardized image set (oasis). *Behavior research methods*, 49(2):457–470, 2017. 6
- [34] W. S. Lages and D. A. Bowman. Walking with adaptive augmented reality workspaces: design and usage patterns. In *Proceedings of the 24th International Conference on Intelligent User Interfaces, IUI '19*, pp. 356–366. Association for Computing Machinery, New York, NY, USA, 2019. 2
- [35] A. Lammert, G. Rendle, F. Immohr, A. Neidhardt, K. Brandenburg, A. Raake, and B. Froehlich. Immersive study analyzer: Collaborative immersive analysis of recorded social vr studies. *IEEE Transactions on Visualization and Computer Graphics*, 2024. 2
- [36] S. M. Lundberg and S.-I. Lee. A unified approach to interpreting model predictions. *Advances in neural information processing systems*, 30, 2017. 8
- [37] W. Luo, A. Lehmann, H. Widengren, and R. Dachsel. Where should we put it? layout and placement strategies of documents in augmented reality for collaborative sensemaking. In *Proceedings of the 2022 CHI Conference on Human Factors in Computing Systems*, pp. 1–16, 2022. 1, 2
- [38] H. Ma, Z. Zhang, W. Li, and S. Lu. Unsupervised human activity representation learning with multi-task deep clustering. *Proceedings of the ACM on Interactive, Mobile, Wearable and Ubiquitous Technologies*, 5(1):1–25, 2021. 5
- [39] K. Mahadevan, Q. Zhou, G. Fitzmaurice, T. Grossman, and F. Anderson. Tesseract: Querying spatial design recordings by manipulating worlds in miniature. In *Proceedings of the 2023 CHI Conference on Human Factors in Computing Systems*, pp. 1–16, 2023. 2
- [40] F. Mathis, B. A. Myers, B. Lafreniere, M. Glueck, and D. P. S. Marques. MR-Driven Near-Future Realities: Previewing Everyday Life Real-World Experiences Using Mixed Reality. In *Proceedings of the 26th International Conference on Multimodal Interaction, ICMI '24*, pp. 76–85. Association for Computing Machinery, New York, NY, USA, Nov. 2024. 1
- [41] A. Matvienko, F. Müller, D. Schön, P. Seesemann, S. Günther, and M. Mühlhäuser. Bikear: Understanding cyclists' crossing decision-making at uncontrolled intersections using augmented reality. In *Proceedings of the 2022 CHI Conference on Human Factors in Computing Systems*, pp. 1–15, 2022. 2
- [42] F. McGee, R. McCall, and J. Baixaulli. Comparison of spatial visualization techniques for radiation in augmented reality. In *Proceedings of the 2024 CHI Conference on Human Factors in Computing Systems*, pp. 1–15, 2024. 1
- [43] Meta. Import Meta XR Packages | Meta Horizon OS Developers, 2024. 6
- [44] Meta. Meta Quest Pro: Premium Mixed Reality | Meta Store, 2024. 6
- [45] D. L. Mills. Internet time synchronization: the network time protocol. *IEEE Transactions on communications*, 39(10):1482–1493, 2002. 3
- [46] J. L. Moreno. Foundations of sociometry: An introduction. *Sociometry*, pp. 15–35, 1941. 2, 3
- [47] M. Nebeling, M. Speicher, X. Wang, S. Rajaram, B. D. Hall, Z. Xie, A. R. Raistrick, M. Aebersold, E. G. Happ, J. Wang, et al. Mrat: The mixed reality analytics toolkit. In *Proceedings of the 2020 CHI Conference on human factors in computing systems*, pp. 1–12, 2020. 2
- [48] D. O. Olguin, P. A. Gloor, and A. S. Pentland. Capturing individual and group behavior with wearable sensors. In *Proceedings of the 2009 aaai spring symposium on human behavior modeling, SSS*, vol. 9, 2009. 2
- [49] P. Paulus. Groups, teams, and creativity: The creative potential of idea-generating groups. *Applied psychology*, 49(2):237–262, 2000. 1
- [50] A. S. Pentland. The new science of building great teams. *Harvard business review*, 90(4):60–69, 2012. 2, 3
- [51] M. C. Potter, B. Wyble, C. E. Hagmann, and E. S. McCourt. Detecting meaning in RSVP at 13 ms per picture. *Attention, Perception & Psychophysics*, 76(2):270–279, Feb. 2014. 4
- [52] S. Puntambekar and R. Luckin. Documenting collaborative interactions: issues and approaches. pp. 737–738, 2023. 2
- [53] D. Romero, R. J. Patel, A. Markopolou, and S. Elmalaki. Gaitguard: Towards private gait in mixed reality. *arXiv preprint arXiv:2312.04470*, 2023. 2
- [54] A. Rorissa and S. K. Hastings. Free sorting of images: Attributes used for categorization. *Proceedings of the American Society for Information Science and Technology*, 41(1):360–366, 2004. 6
- [55] M. L. Rusch, M. C. Schall, P. Gavin, J. D. Lee, J. D. Dawson, S. Vercera, and M. Rizzo. Directing driver attention with augmented reality cues. *Transportation Research Part F: Traffic Psychology and Behaviour*, 16:127–137, Jan. 2013. 2
- [56] J. A. Russell. A circumplex model of affect. *Journal of Personality and Social Psychology*, 39(6):1161–1178, Dec. 1980. 6
- [57] H. Sacks, E. A. Schegloff, and G. Jefferson. A simplest systematics for the organization of turn-taking for conversation. *language*, 50(4):696–735, 1974. 3
- [58] J. Scott. Social network analysis: developments, advances, and

- prospects. *Social network analysis and mining*, 1:21–26, 2011. 5
- [59] E. Shriberg. Phonetic consequences of speech disfluency. In *Proceedings of the international congress of phonetic sciences*, vol. 1, p. 2, 1999. 4
- [60] H. Stefanidi, M. Tatzgern, and A. Meschtscherjakov. Augmented Reality on the Move: A Systematic Literature Review for Vulnerable Road Users. *Proc. ACM Hum.-Comput. Interact.*, 8(MHCI):245:1–245:30, Sept. 2024. 2
- [61] R. M. Stogdill. Group productivity, drive, and cohesiveness. *Organizational behavior and human performance*, 8(1):26–43, 1972. 1
- [62] K. A. Szczurek, R. M. Prades, E. Matheson, J. Rodriguez-Nogueira, and M. D. Castro. Multimodal Multi-User Mixed Reality Human–Robot Interface for Remote Operations in Hazardous Environments. *IEEE Access*, 11:17305–17333, 2023. 1, 2
- [63] H. Tajfel and J. C. Turner. The social identity theory of intergroup behavior. In *Political psychology*, pp. 276–293. Psychology Press, 2004. 2
- [64] T. Q. Tran, T. Langlotz, and H. Regenbrecht. A Survey On Measuring Presence in Mixed Reality. In *Proceedings of the 2024 CHI Conference on Human Factors in Computing Systems*, CHI '24, pp. 1–38. Association for Computing Machinery, New York, NY, USA, May 2024. 1
- [65] I. S. University. 8.2 Defining Small Groups and Teams. Book Title: Introduction to Public Communication Publisher: Originally published by Indiana State University. 6
- [66] R. Vertegaal. The GAZE groupware system: mediating joint attention in multiparty communication and collaboration. In *Proceedings of the SIGCHI conference on Human Factors in Computing Systems*, CHI '99, pp. 294–301. Association for Computing Machinery, New York, NY, USA, May 1999. 3
- [67] G. Vissers and B. Dankbaar. Knowledge and Proximity. *European Planning Studies*, 21(5):700–721, May 2013. 3
- [68] S. Wasserman and K. Faust. Social network analysis: Methods and applications. 1994. 2
- [69] D. J. Watts and S. H. Strogatz. Collective dynamics of ‘small-world’ networks. *nature*, 393(6684):440–442, 1998. 5
- [70] D.-S. Yang, E. FitzGibbon, and F. Miles. Short-latency disparityvergence eye movements in humans: sensitivity to simulated orthogonal tropias. *Vision Research*, 43(4):431–443, 2003. 3
- [71] Y. Yang, T. Dwyer, M. Wybrow, B. Lee, M. Cordeil, M. Billinghurst, and B. H. Thomas. Towards Immersive Collaborative Sensemaking. *Proceedings of the ACM on Human-Computer Interaction*, 6:722–746, Nov. 2022. 2, 3
- [72] C. Yin, S. Zhang, J. Wang, and N. N. Xiong. Anomaly detection based on convolutional recurrent autoencoder for iot time series. *IEEE Transactions on Systems, Man, and Cybernetics: Systems*, 52(1):112–122, 2020. 5
- [73] N. Yuill, S. Hinske, S. E. Williams, and G. Leith. How getting noticed helps getting on: successful attention capture doubles children’s cooperative play. *Frontiers in Psychology*, 5, May 2014. 3
- [74] X. Zhang, X. Bai, S. Zhang, W. He, P. Wang, Z. Wang, Y. Yan, and Q. Yu. Real-time 3d video-based mr remote collaboration using gesture cues and virtual replicas. *The International Journal of Advanced Manufacturing Technology*, 121(11):7697–7719, 2022. 1
- [75] Y. Zhang, J. Olenick, C.-H. Chang, S. W. Kozlowski, and H. Hung. Teamsense: assessing personal affect and group cohesion in small teams through dyadic interaction and behavior analysis with wearable sensors. *Proceedings of the ACM on Interactive, Mobile, Wearable and Ubiquitous Technologies*, 2(3):1–22, 2018. 1, 2, 3
- [76] T. Zhao, M. Taherisadr, and S. Elmaliaki. Fairo: Fairness-aware sequential decision making for human-in-the-loop cps. In *2024 ACM/IEEE 15th International Conference on Cyber-Physical Systems (ICCPS)*, pp. 87–98. IEEE, 2024. 1